



1 **The impact of wave physics in the CMEMS-IBI ocean system Part A :**
2 **Wave forcing validation.**

3

4 Romain Rainaud⁽¹⁾, Lotfi Aouf⁽¹⁾, Alice Dalphiné⁽¹⁾, Marcos Garcia Sotillo⁽²⁾, Enrique Alvarez-
5 Fanjul⁽²⁾, Guillaume Reffray⁽³⁾, Bruno Levier⁽³⁾, Stéphane LawChune⁽³⁾, Pablo Lorente⁽²⁾, Cristina
6 Toledano⁽⁴⁾

7

⁽¹⁾Météo-France

8

⁽²⁾Puertos del Estado

9

⁽³⁾Mercator-Ocean International

10

⁽⁴⁾Nologin Consulting

11

12

13

Abstract

14

15 The Iberian Biscay Ireland (IBI) wave system has the challenge to improve wave forecast and the
16 coupling with ocean circulation model dedicated to western european coast. The momentum and
17 heat fluxes at the sea surface are strongly controlled by the waves and there is a need of using
18 accurate sea state from wave model. This work describes the more recent version of the IBI wave
19 system and highlight the performance of system in comparison with satellite altimeters and buoys
20 wave data. The validation process has been performed for 1-year run of the wave model MFWAM
21 with boundary conditions provided by the global wave system. The results show on the one hand a
22 slightly improvement on significant wave height and peak period, and on the other hand a better
23 surface stress for high wind conditions. This latter is a consequence of using a tail wave spectrum
24 shaped as the Philipps wave spectrum for high frequency waves.

25

26

27

28

29

30

31

32

33



34

35 **1. Introduction**

36

37 Waves constitute the interface between ocean and atmosphere and have an important role in
38 term of exchanges through this interface (Cavaleri et al., 2012). Their representation is necessary to
39 compute with accuracy the different air-sea fluxes of heat and momentum (Janssen et al., 2004).
40 However, waves are generally parameterized from 10-m local wind. While there is a correlation
41 between wind and waves, their relationship is not exclusive. Indeed, waves are also present without
42 wind and for a given local wind speed, the local wave field is variable (Hanley et al., 2010).
43 Moreover, it is generally accepted that wind directly generates surface currents because about 90%
44 of the wind momentum input to waves is immediately passed to the ocean (Cavaleri et al., 2012). In
45 fact, waves absorb energy and momentum from the wind during their formation and growth, and
46 return it when they break (Breivik et al., 2015). This explains why it is necessary to introduce an
47 accurate sea state description, from wave model (or database as for example Rasclé et al., 2007),
48 which control exchanges between ocean and atmosphere.

49 Waves affect the ocean surface layer through different processes (Breivik et al., 2015) :

- 50 - Waves induce current in surface via the Stokes drift, rapidly attenuated with depth. The Stokes
51 drift velocity associated with the wave fields adds a term on the Coriolis effect in the momentum
52 equation. This process is called Stokes-Coriolis forcing.
- 53 - A part of the atmospheric wind stress is used by waves to grow and is not provided to the ocean.
54 This energy quantity must be subtracted from the oceanic wind stress which drives the ocean model.
- 55 - During wave breaking, turbulent kinetic energy is produced and induces to the ocean surface layer
56 an enhanced turbulent mixing. A more accurate description of these processes will be given in the
57 part B of this study.

58 Recent studies investigated the impact of the wave effect on the representation of the ocean
59 surface layer at different scales of time and space. One of the major impact is the improvement of
60 the Mixed-Layer-Depth (MLD) using wave-induced MLD parametrization (Fan et al., 2014) which
61 lead to an important impact on the atmospheric surface temperature, pressure and precipitation
62 (Babanin et al., 2009, 2012). In a climate scale, this can affect global sea-surface pressure patterns
63 and atmospheric circulation. Breivik et al., (2015) showed that the use of wave forcing in oceanic
64 surface induces a reduction of the global annual SST bias amplitude on a period from 1979 to 2010.
65 They used a coarse 1° horizontal grid resolution of NEMO ocean model and wave forcing from
66 ECWAM wave model. An important reduction of the amplitude of the diurnal cycle of SST and



67 surface current had been exposed by Janssen (2012). At the interface of ocean and atmosphere,
68 waves modify the surface layer and induce an increase of the roughness length, which enhances
69 the wind stress (Thévenot et al., 2016). Ginis (2008) has advised the use of an ocean-waves-
70 atmosphere coupled system to improve the representation of tropical cyclones intensity, structure
71 and trajectories. Indeed, Chunxia et al., (2008) studied the effect of sea waves during typhoon
72 Imodu (15-19 July 2003). They found that the waves had a small effect on the typhoon track but
73 they revealed a relation between wave age and 10-m wind speed inducing impact on air-sea fluxes
74 and precipitations. These changes obviously affect the oceanic surface layer behavior. The high-
75 resolution NEMO-WAM system had been used by Staneva et al. (2017) for the Baltic and North
76 Sea. They showed that when using a wave forcing on the ocean surface induces a Sea Surface
77 Temperature (SST) closer to the one provided by MODIS satellite than without wave forcing. The
78 NEMO-WAM system was also in better agreement with sea surface height and surface current
79 observations during the Xaver storm event (06 December 2014).

80 The Copernicus Marine Environmental Monitoring Service (CMEMS) is a strong European
81 partnership with more than 50 marine operational and research centers in Europe involved in the
82 marine monitoring and forecasting services. It provides a wide range of marine products of social
83 and environmental value such as ocean currents, temperature, salinity, sea level, pelagic
84 biogeochemistry and waves. The Monitoring Forecasting System (MFC) generates model-based
85 products including analysis of the current situation, forecasts of the situation a few days in advance
86 and the delivery of retrospective data records (re-analysis). In order to increase the quality of these
87 ocean products, an evaluation of the impact of wave forcing on oceanic surface layer is needed.
88 Météo-France has implemented the coupling between the wave model MFWAM and the ocean
89 model NEMO. This aims to provide reference and accurate physical oceanic state on Iberian-
90 Biscay-Irish (IBI, Figure 1) ocean area. . The goal of this paper is to evaluate the impact of waves
91 forcing on ocean circulation for IBI ocean area during the year 2014, where there were a by several
92 storms events. Validation and analysis on oceanic key parameters was performed in preparation of
93 using NEMO V4 IBI-Wave system in the operational Copernicus CMEMS-IBI-MFC.

94 This study is splitted in two parts. The part A described in this paper, is dedicated to the
95 MFWAM validation and is structured as follow. First, a description of the wave model MFWAM is
96 given in section 2. Section 3 indicates a the different wave observations and performed model runs.
97 Results on the validation is given at Section 4. Finally, a summary and concluding remarks will
98 discussed in Section 5. The part B of this paper describes the impact of the wave forcing on the
99 ocean circulation model.

100



101 **2. Description of the wave Model MFWAM**

102

103 The wave model of Météo-France MFWAM provides the mean wave parameters for the
104 Copernicus Marine Environment and Monitoring Service (CMEMS) for Iberian-Biscay-Ireland seas
105 domain. The model is based on the ECWAM-IFS38R2 computing code (ECMWF 2013) with two
106 major changes related to the dissipation source terms. The model MFWAM uses the physics
107 developed in Ardhuin et al. (2010) which is called ST4. The MFWAM model takes also into
108 account a swell damping term related to the air friction at the sea surface. Recently the model has
109 been upgraded with adjustment of the dissipation source terms and also improvement on drag
110 limitation by using a tail shape from the Philipps wave spectrum (Janssen et al. 2014). Table 1
111 gives the tuned coefficients of ST4 physics for the old and new version of the model referred to as
112 V3 and V4, respectively. In this study the model MFWAM is set for a IBI domain (25°N to 64.6°N
113 in latitude) with a grid size of 0.10°. The model uses a bathymetry from ETOPO2 and is driven by
114 6-hourly analyzed winds from the IFS-ECMWF atmospheric model. The wave spectrum is
115 discretized in 24 directions and 30 frequencies starting from 0.035 to 0.57 Hz with increasing step
116 of 1.1. The boundary conditions are provided from the global model MFWAM run with a time step
117 of 3 hours. The data assimilation is not activated for this study.

118

119 **3. Observations and model runs**

120 **3.1 Wave observations**

121 *Satellite data*

122 Two different SST satellite products, OSTIA and L3S have been used in this study. The
123 OSTIA daily product of SST is a level 4 multi-sensor product at a resolution of 0.02° built by using
124 optimal interpolation from several satellite missions such as AVHRR_METOP_B,
125 SEVIRI*VIIRS_NPP, AVHRR_19, AVHRR_18, MODIS_A, MODIS_T, AMSR2. The
126 hierarchy can be changed in time depending on the health of each sensor. The L3S product consists
127 in a fusion of daily SST observations from multiple satellite sensors, over a 0.1° resolution grid. It
128 includes observations by polar orbiting (NOAA-18 & NOAA-19/AVHRR, METOP-A/AVHRR,
129 ENVISAT/AATSR, AQUA/AMSRE, TRMM/TMI) and geostationary (MSG/SEVIRI, GEOS-11)
130 satellites. The observations of each sensor are intercalibrated prior to merging using a bias
131 correction based on a multi-sensor median reference correcting the large scale cross-sensor biases.

132 Satellite observations of significant wave height (SWH) for the year 2014 are provided by



133 altimeters missions JASON-2 and SARAL. Altimeters SWH are interpolated in a box with a grid
134 size of 0.1° and collocated with model MFWAM SWH with a time window of 3 hours.

135 Level 4 surface currents satellite data are from altimeter satellite gridded sea surface heights
136 and derived variables. This product is processed by the SL-TAC multimission altimeter data
137 processing system. It processes data from all altimeter missions: Jason-3, Sentinel-3A, HY-2A,
138 Saral/AltiKa, Cryosat-2, Jason-2, Jason-1, T/P, ENVISAT, GFO, ERS ½. It provides a consistent
139 and homogeneous catalogue of products for varied applications, both for near real time applications
140 and offline studies. The resolution of the product is 0.25° .

141

142 *Wave buoys*

143 In-situ buoys are also used to evaluate model outputs. These buoys provide data of surface
144 atmosphere, wave and ocean parameters. Data are from the network of Puertos del Estado for
145 spanish buoys, Météo France for french buoys and from irish buoys. The Table 2 and Figure 1
146 summarize the names, locations, nationality and reference code used in the following for the
147 different buoys.

148

149

150 **3.2. Wave model runs**

151

152 The first wave experiment, called MFWAM-V3, was performed with the version 3 of the
153 MFWAM-IBI code. One year run of the model has been performed starting from 27 November
154 2013, until 31 December 2014. The wave model is driven by 6-hourly analysed wind forcing from
155 ECMWF-IFS atmospheric system. The boundary conditions are provided every 3 hours by a global
156 MFWAM model run with a grid resolution of 0.5° .

157 The second wave experiment, called MFWAM-V4, is performed with the most recent
158 version 4 of the MFWAM-IBI code. This latter has an adjustment of the dissipation source term in
159 order to improve the surface stress for high winds. the physics parameter settings include the
160 sheltering parameter S_u , non-dimensional growth parameter β_{max} , the dissipation coefficient C_{ds}
161 (a negative constant). Also a tail factor was reduced in order to account the Phillips wave spectrum
162 for high frequency waves. These parameters are calibrated following the ST4 physics developed in
163 Ardhuin et al. (2010). Table 2 summarizes physical settings of the two model MFWAM versions 3
164 and 4.

165 Figures 2a and 2b show the variation of the surface drag coefficient with 10-meter wind speed. It is
166 clearly observed that the MFWAM V4 reduces significantly the drag coefficient for high wind



167 speed larger than 20 m/s. The scatter diagram shows more consistent sea state dependency from the
168 model V4 than V3.

169 Significant wave heights provided by the wave model runs are validated by comparison with
170 altimeters satellite wave data for the entire year 2014. The wave forcing provided to ocean model
171 NEMO includes the following parameters : significant wave height, drag coefficient, Stokes
172 velocity components, mean wave period, and wave number, normalized wind stress, Craig and
173 Banner coefficient, energy flux and significant height of wind waves. The impact of these
174 parameters on the ocean surface will be investigated in the part B of the study.

175

176 **4. Validation of the wave output fields**

177

178 The validation of the wave model MFWAM is based on a statistical analysis of significant wave
179 heights from the model compared to altimeter wave data (JASON-2 and Saral/Altika), as mentioned
180 in previous section. Metrics used in this study are normalized scatter index and bias. Figure 3 shows
181 the scatter plots of SWH from altimeters and models for the year 2014. This reveals a slightly better
182 slope for V4, but overall good performance of the MFWAM-IBI wave model for V3 and V4
183 versions. The scatter index of SWH is roughly of 12.5% and the bias is negative and roughly 15
184 cm. The model MFWAM underestimates SWH which is mostly induced by the underestimation of
185 the surface wind speed from the atmospheric model in the IBI domain. Table 3 highlights the very
186 good and close performance of both versions during 2014. Figure 4 and 5 show maps of average
187 scatter index and bias on the IBI domain, respectively. Most of scatter index are ranged between 8
188 to 15% depending on the ocean area. However, we can mention that wave model V3 and V4 have a
189 better skill on the Atlantic ocean than on North and Mediterranean seas. The maps of bias also show
190 a general underestimation of SWH except on Gulf of Biscay where the model MFWAM induced an
191 overestimation of SWH for both V3 and V4. A detail analysis is given by the monthly variation of
192 the model performance, as illustrated in figure 6. For V3 and V4 versions, the scatter index is
193 ranging between 11 and 14% during all the year, which indicates that the good performance of the
194 MFWAM-IBI wave model is for the entire year. Monthly scatter index are slightly better for
195 MFWAM-V4, which confirms the better performance of this version on the IBI domain.

196 Performances of the model MFWAM are also investigated depending on regional domains.
197 Three domains have been selected depending on latitudes as indicated in figure 8. Zone 1 concerns
198 latitudes between 25°N-35°N (called Canarias domain), while Zone 2 considers latitudes 35°N-
199 49°N (called Spain-France domain). Zone 3 accounts for northern latitudes ranging between 49°N-
200 64.5°N (called GB-Ireland domain). For all zones during 2014, the scatter index and bias of SWH is



201 ranging between 12% and 13% and between -10 cm and -20 cm, respectively. One can indicate that
202 the scatter index of SWH is better for zones 1 and 3 while the bias is better for zone 2 during 2014.
203 Table 4 shows also a slightly better performance for MFWAM-V4, in particular for the scatter
204 index, for the three zones. This confirms what was previously mentioned concerning differences
205 between the two versions. Figure 8 shows monthly scatter index and bias during 2014 for the three
206 ocean zones. The scatter index of SWH is ranging between 10% and 15% and the best performance
207 is obtained during summer for months June and July. While during winter with intense storms in
208 North Atlantic ocean the scatter index of SWH is larger for zones 2 and 3.

209 The significant wave height from MFWAM runs has also been evaluated with buoys
210 measurements. Histograms of Figure 9 show the monthly scatter index during 2014. At BelmA
211 buoy, the scatter index is lower than 15% during the entire year except on June and November.
212 Moreover, the performance of the two runs is globally the same during all the year despite a slightly
213 increase of MFWAM-V4. However, at BI buoy, the performance of MFWAM-V4 is generally
214 better MFWAM-V3 during the entire year. At this location, the scatter index oscillate between 10%
215 and 20% because of storm occurrence in this area.

216 The validation of the MFWAM V3 and V4 has indicated good skills during the year 2014.
217 This opens the use of accurate description of the sea state and consequently good wave forcing to
218 drive the ocean model NEMO. Moreover, in term of differences between MFWAM-V3 and
219 MFWAM-V4, the validation showed an general increase of the quality thanks to the physical
220 settings of MFWAM-V4.

221

222 5-Conclusions

223

224 The wave model MFWAM V4 version has been upgraded with physical adjustments that induced a
225 more consistent surface stress dependency with 10-meter wind speed. The use of tail shape of
226 Philipps spectrum also induces a better high frequency waves and consequently a better estimate of
227 Stokes drift. The validation with altimeters wave data has been shown a slight improvement of bias
228 and scatter index over IBI domain. The model MFWAM induces a negative bias that indicate an
229 underestimation of significant wave height mostly because of uncertainties related to strong winds
230 during winter and fall season from the ECMWF atmospheric system. The bias of significant wave
231 height in summer season is small roughly less than 5 cm. The regional statistical analysis has
232 revealed the best improvement of the model MFWAM V4 on the zone 2 which includes portuguese,
233 spanish and french coasts. The validation with buoys has indicated a significant improvement of
234 SWH at Belle-ile buoys located in coastal area of brittany french coast.



235 The model MFWAM V4 is suited to well describe surface stress, stokes drift and the dissipation by
236 wave breaking inducing turbulence in the ocean mixed layer.

237

238 **References**

239

240 Ardhuin, F., Rogers E., Babanin A., Filipot J-F., Magne R., Roland A., Van der Westhuysen A,
241 Queffeulou P., Lefevre J.-M., Aouf L., Collard F. : Semi-empirical dissipation source functions for
242 wind-wave models: part I, definition, calibration and validation, *Journal of Physical Oceanography*,
243 Volume 40, pp1917-1941, <https://doi.org/10.1175/2010JPO4324.1>, 2010.

244 Babanin, A., Onorato M., Qiao, F. : Surface waves and wave-coupled effects in lower atmosphere
245 and upper ocean, *Journal of Geophysical Research.*, 117, C11,
246 <https://doi.org/10.1029/2012JC007932>, 2012.

247 Babanin, A. V., Ganopolski A., Phillips W. R. C. : Wave-induced upper-ocean mixing in a climate
248 model of intermediate complexity. *Ocean Modelling*, 29, 189–197,
249 <https://doi.org/10.1016/j.ocemod.2009.04.003>, 2009.

250 Breivik, O., Mogensen K., Bidlot J., Balmaseda M., Janssen P. : Surface wave effects in the NEMO
251 ocean model : Forced and coupled experiments, *Journal of Geophysical Research*, Volume 120,
252 issue 4, 2973-2992, <https://doi.org/10.1002/2014JC010565>, 2015.

253 Cavaleri, L., Fox-Kemper B., Hemer M. : Wind waves in the climate coupled system. *Bulletin of*
254 *American Meteorological Society*, 1651-1661, <https://doi.org/10.1175/BAMS-D-11-00170.1>, , 2012.

255 Chunxia L., QuanqI Y., Liang L. : The effect of sea waves on the typhoon Imodu, *Proceeding of*
256 *High Resolution Modelling CAWCR workshop*, Melbourne, Australia, 25-28 November 2008.

257 Fan, Y., and S. M. Griffies S. M. : Impacts of parameterized Langmuir turbulence and nonbreaking
258 wave mixing in global cli-mate simulations. *Journal of Climate*, 27, 4752–4775,
259 <https://doi.org/10.1175/JCLI-D-13-00583.1>, 2014

260 Ginis, I. : Atmophere-Ocean coupling in tropical cyclone, *Proceedings of ECMWF workshop on*
261 *Ocean-Atmosphere interactions*, Reading, UK, 10-12 November, 2008.

262 Hanley, K. E., Belcher S. E., Sullivan P. P. : A global climatology of wind-wave interaction. *J.*
263 *Phys. Oceanogr.*, 40, 1263–1282, <https://doi.org/10.1175/2010JPO4377.1>, 2010.

264 Janssen, P. A. E. M., 2004 : *The Interaction of Ocean Waves and Wind*. Cambridge University
265 Press.

266 Janssen, P. A. E. M. : Ocean wave effects on the daily cycle in SST, *J. Geophys. Res.*, 117, C00J32,
267 <https://doi.org/10.1029/2012JC007943>, 2012.



268 Janssen, P. A. E. M., Aouf, L., Behrens, Breivik, O., A., Korres, G., Cavalieri, L., Christensen, K.,
269 : Final report of work-package I of 7th Framework Program Mywave project. European
270 Commission, December 2014.

271 Rasclé, N., Ardhuin, F., Queffelec, P., Croizé-Fillon, D. : A global wave parameter database for
272 geophysical applications. Part 1: wave-current-turbulence interaction parameters for the open ocean
273 based on traditional parameterizations. *Ocean Modelling* 25, 154–
274 171, <https://doi.org/10.1016/j.ocemod.2008.07.006>, 2008.

275 Staneva J., Alari V., Breivik O, Bidlot J.-R. and Mogensen K. : Effects of wave-induced forcing on
276 a circulation model of the North Sea. *Ocean Dynamics*, Vol. 67, Issue 1, 81-191,
277 <https://doi.org/10.1007/s10236-016-1009-0>, 2017

278 Thevenot, O., M-N. Bouin, V. Ducrocq, C. Lebeaupin-Brossier, O. Nuissier, J. Pianezze, F.
279 Duffourg : Influence of the sea state on Mediterranean heavy precipitation : A case study from
280 Hymex-SOP-1, *Quarterly Journal of the Royal Meteorological Society*, Volume 142, Issue S1,
281 Pages 377-389, <http://doi.org/10.1002/qj.2660>, 2016.

282

283

284

285

286

287

288

289

290

291

292

293

294

295

296

297

298

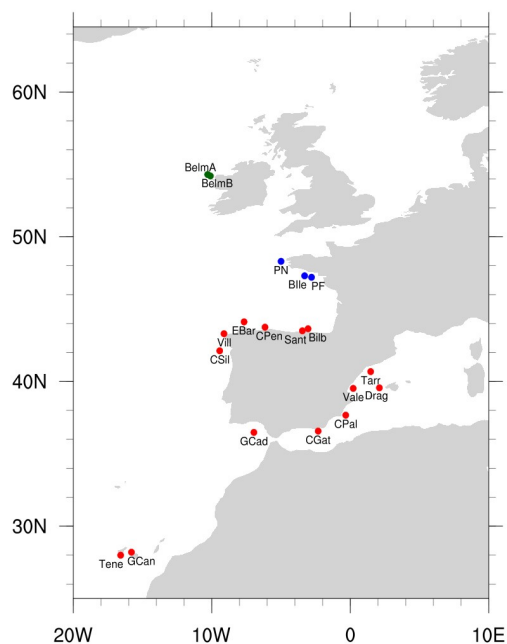


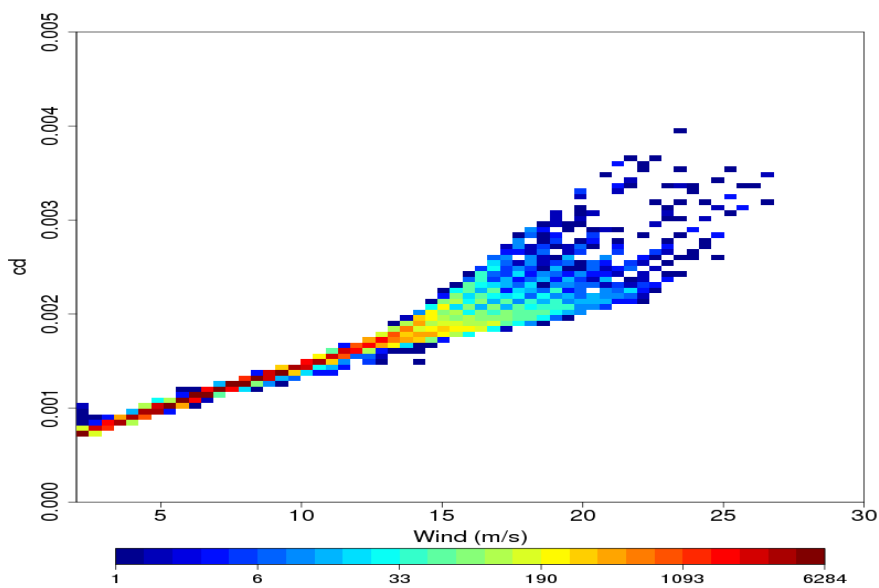
Figure 1 : Name and location of buoys in the IBI domain.

300
301
302
303
304
305
306
307
308
309
310
311
312
313
314
315
316



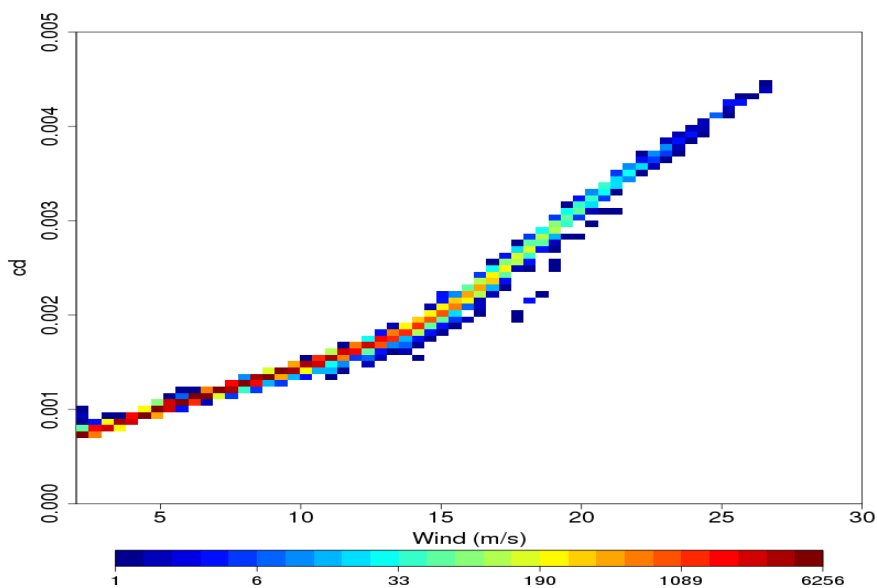
317

(a)



319

(b)



321

322 Figure 2 : Scatter diagram of drag coefficient from model runs with 10-meter wind speed during
323 2014. (a) and (b) stand for MFWAM-V4 and V3, respectively.



324

325

326

327

328

329

330

331

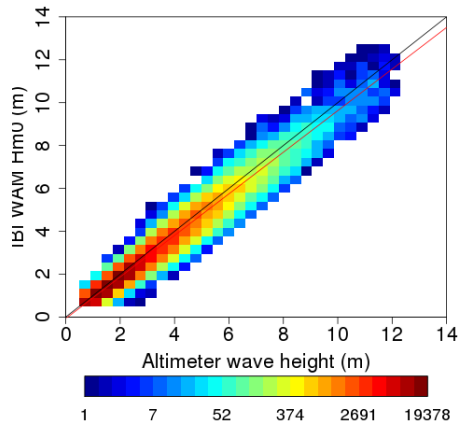
332

333

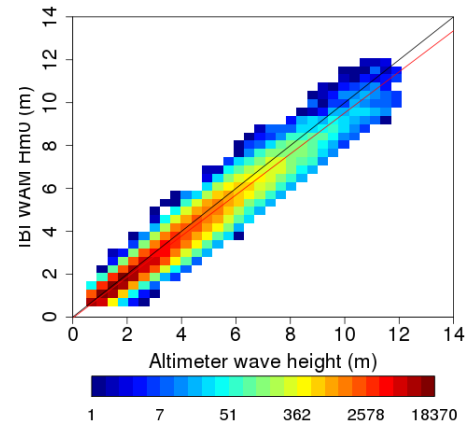
334

335

336



(a)



(b)

338 Figure 3 : Scatter plots of significant wave heights from model and altimeters during 2014. (a) and
339 (b) stand for MFWAM-V3 and MFWAM-V4, respectively. Satellite altimeters are JASON-2 and
340 SARAL.

341

342

343

344

345

346

347

348

349

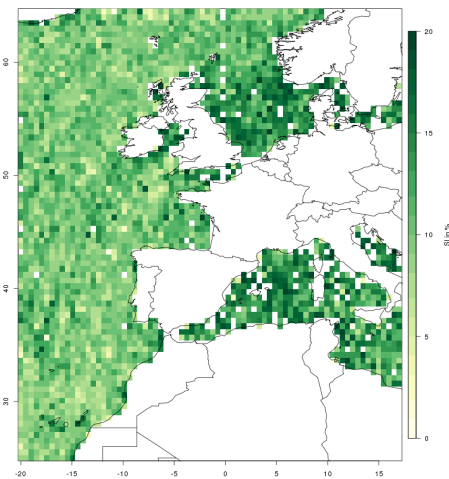
350

351

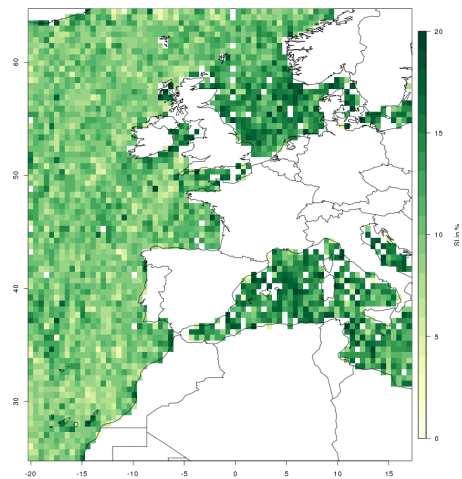
352

353

354



(a)



(b)

355 Figure 4 : Normalized scatter index of significant wave height for IBI ocean domain during 2014.
356 (a) and (b) stand for MFWAM-V3 and MFWAM-V4, respectively. Comparison has been performed
357 with altimeters Jason-2 and SARAL.



358
 359
 360
 361
 362
 363
 364
 365
 366
 367
 368
 369
 370
 371
 372
 373
 374

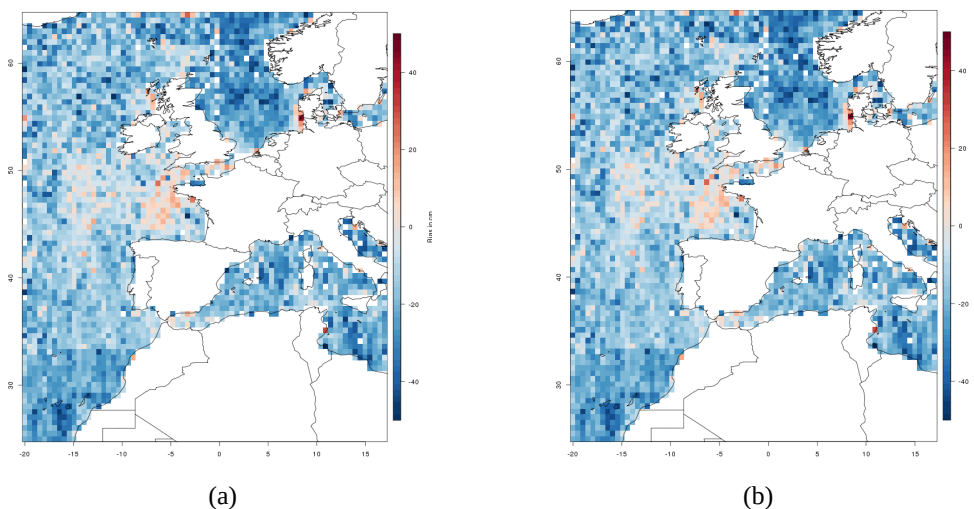


Figure 5 : Bias of significant wave height for IBI ocean domain during 2014. (a) and (b) stand for MFWAM-V3 and MFWAM-V4. Comparison has been performed with altimeters Jason-2 and SARAL.

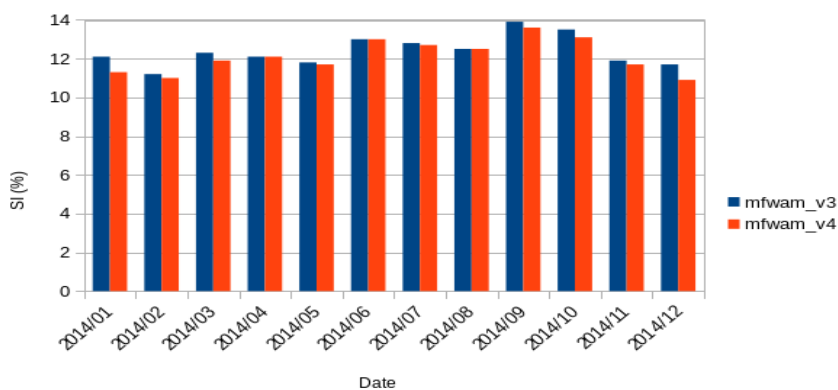


Figure 6 : Monthly evolution of the normalized scatter index of SWH from model MFWAM during 2014. Blue and red histogram bars indicate MFWAM-V3 and MFWAM-V4, respectively.

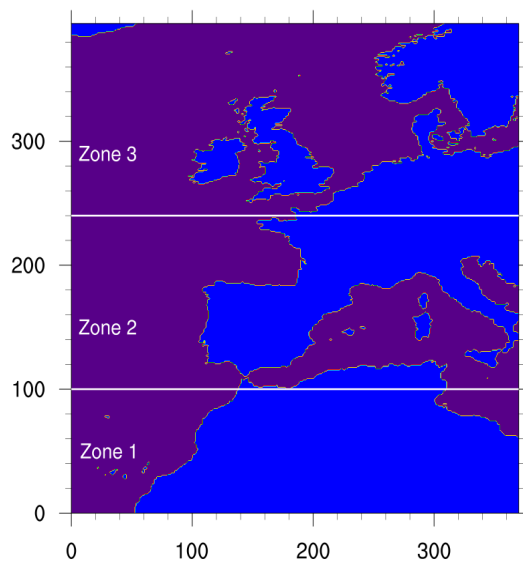


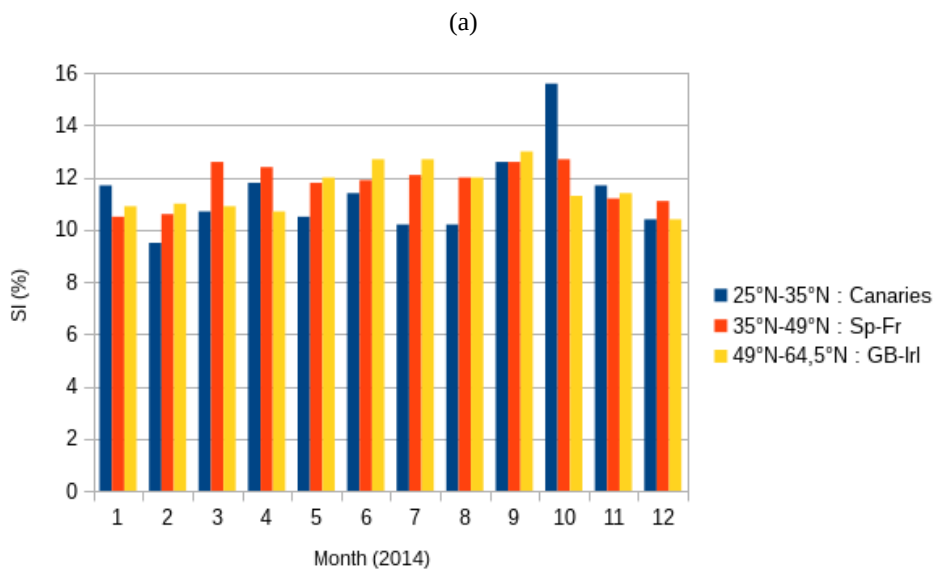
Figure 7 : Regional domains for the validation of IBI wave heights.

380
381
382
383
384
385
386
387
388
389
390
391
392
393
394
395
396
397
398
399

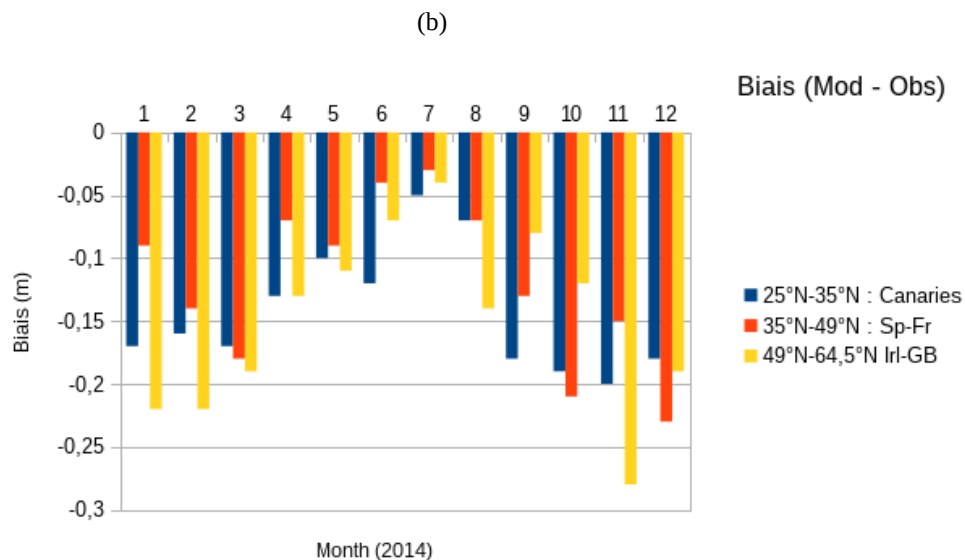


400

401



402



403

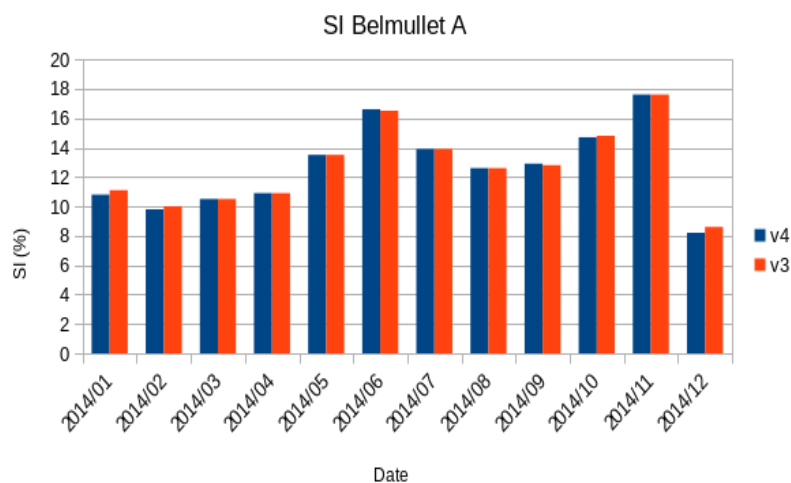
404 Figure 8 : monthly variations of statistical parameters during 2014. (a) and (b) stand for normalized
 405 scatter index of SWH and bias, respectively. Blue, red and yellow histogram bars indicate zone 1,
 406 zone 2 and zone 3, respectively.

407



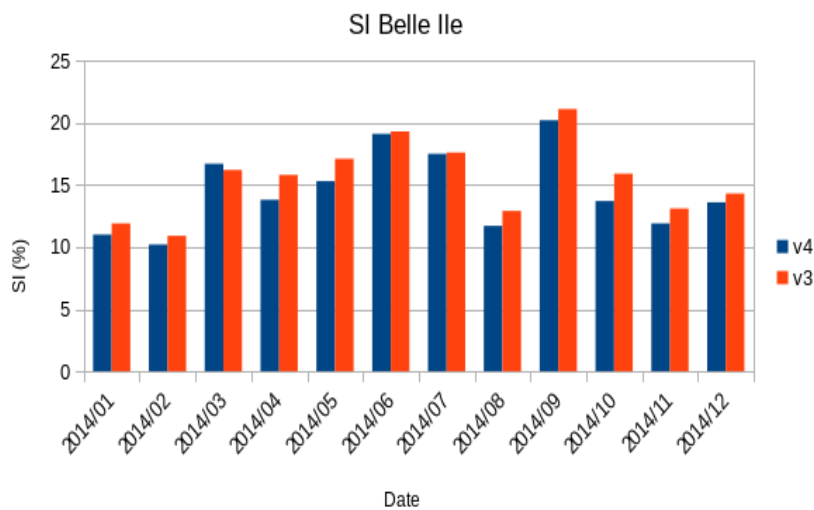
408

(a)



410

(b)



412

413 Figure 9 : Monthly variation of normalized scatter index of SWH during 2014 at buoys BelmaA in
414 (a) and Belle ile in (b). Red and blue histogram bars stand for MFWAM-V3 and MFWAM-V4,
415 respectively.



416

417

| | Cds | Su | β_{max} | Tail Factor |
|-----------------|----------------------|-----------|---------------------------------|--------------------|
| MFWAM-V3 | $-2.8 \cdot 10^{-5}$ | 0.6 | 1.52 | 9.9 |
| MFWAM-V4 | $-2.6 \cdot 10^{-5}$ | 0.4 | 1.48 | 4.0 |

418

419

Table 1 : Values of the model settings of MFWAM V3 and V4 versions.

420

| Buoy name | Location | Reference code | Nationality |
|-------------------------|-----------------|-----------------------|--------------------|
| Bilbao Vizcaya | 43.64°N 3.05°W | Bilb | Spanish |
| Cabo de Gata | 36.57°N 2.32°W | CGat | Spanish |
| Cabo de Palos | 37.67°N 0.33°W | CPal | Spanish |
| Cabo Penhas | 43.75°N 6.16°W | CPen | Spanish |
| Cabo Silleiro | 42.12°N 9.43°W | CSil | Spanish |
| Drogonera | 39.56°N 2.10°E | Drog | Spanish |
| Estaca Bares | 44.12°N 7.67°W | EBar | Spanish |
| Golfo de Cadiz | 36.48°N 6.96°W | GCad | Spanish |
| Gran Canaria | 28.20°N 15.80°W | GCan | Spanish |
| Tarragona | 40.68°N 1.47°E | Tarr | Spanish |
| Tenerife | 27.99°N 16.58°W | Tene | Spanish |
| Valencia | 39.52°N 0.21°E | Vale | Spanish |
| Villano Sisargas | 43.3°N 9.12°W | Vill | Spanish |
| Santander | 43.50°N 3.46°W | Sant | Spanish |
| Belle Ile | 47.30°N 3.30°W | BI | French |
| Pierre Noire | 48.30°N 5.00°W | PN | French |
| Plateau du Four | 47.20°N 2.80°W | PF | French |
| Belmullet A | 54.28°N 10.27°W | BelmA | Irish |
| Belmullet B | 54.23°N 10.14°W | BelmB | Irish |

421

422

Table 2 : Name, location, nationality and reference code of the moored buoys.

423

424

425

426

427



428

429

430

| | MFWAM-V3 | MFWAM-V4 |
|--------------------------|-----------------|-----------------|
| Scatter Index (%) | 12,6 % | 12,5 % |
| Bias (m) | -0,15 m | -0,15 m |

431

432

Table 3 : Scatter index and bias for year 2014 and for the two versions of MFWAM.

433

434

| | MFWAM-V3 | | | MFWAM-V4 | | |
|-----------------|-----------------|---------------|---------------|-----------------|---------------|---------------|
| | Zone 1 | Zone 2 | Zone 3 | Zone 1 | Zone 2 | Zone 3 |
| SI (%) | 12.4 | 12.7 | 12.4 | 12.3 | 12.6 | 12.3 |
| Bias (m) | -0.18 | -0.12 | -0.16 | -0.18 | -0.12 | -0.16 |

435

436

Table 4 : Normalized scatter Index and biases of SWH from MFWAM V3 and V4 during 2014 for

437

the ocean domains described on Figure 7.